Evaluation of Quantitative Probes for Weaker Cu(I) Binding Sites Completes a Set of Four Capable of Detecting Cu(I) Affinities from Nanomolar to Attomolar

Zhiguang Xiao,* Lisa Gottschlich, Renate van der Meulen, Saumya R Udagedara and Anthony G Wedd

School of Chemistry, Bio21 Molecular Science and Biotechnology Institute, University of Melbourne, Parkville, Victoria 3010, Australia

Email: z.xiao@unimelb.edu.au

Tel (61 3) 8344 2377

Fax (61 3) 9347 5180

Supplementary Information

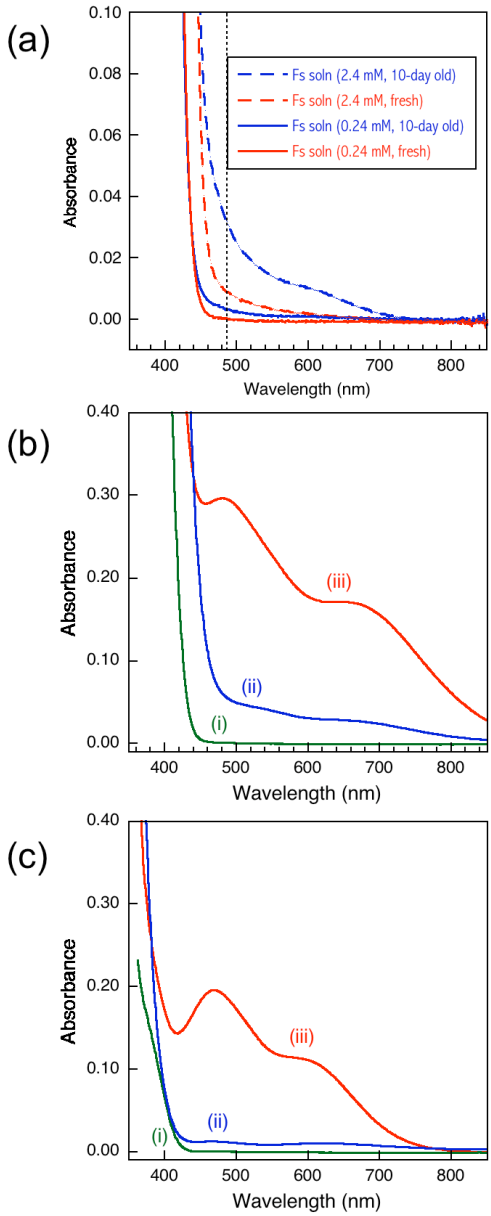

Fig S1. (a) Solution spectra of Fs ligand (2.4 mM in dash lines and 0.24 mM in solid lines; fresh solutions in **red** and 10-day old solutions in **blue**) in Mops buffer (50 mM, pH 7.0); (b, c) (i) Solution spectra in Mops buffer (50 mM, pH 7.0) of fresh ligand L (270 μM; L = Fs for (b) and L = Fz for (c)); (ii) spectra after addition of $Cu^{II}SO_4$ (45 μM) into solution (i); (iii) spectra after addition of NH_2OH (2.0 mM) and Asc (1.0 mM) into solution (ii).

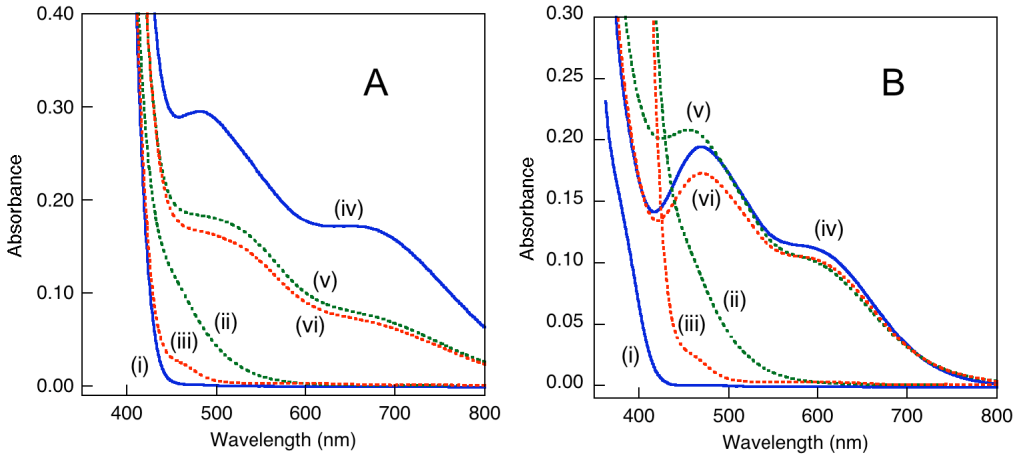

Fig S2. Effects of dithionite on the solution spectra of ligand L and complex $[Cu^{I}L_2]^{3-}$ in Mops buffer (50 mM, pH 7.0) (A: L = Fs; B: L = Fz):

(i) Spectrum of a solution containing ligand L only (270 μM);

(ii) Spectrum of a solution containing ligand L (270 μM) and Dit (1.0 mM) (note: Dit has no absorbance at $\lambda > 400$ nm);

(iii) Spectrum of the solution (ii) after a brief bubbling of air;

(iv) Spectrum of a solution containing $[Cu^{I}L_2]^{3-}$ prepared by mixing $CuSO_4$ (45 μM), L (270 μM) and NH_2OH (2.0 mM) in Mops (50 mM, pH 7.0);

(v) Spectrum of the solution (iv) after inclusion of Dit (1.0 mM);

(vi) Spectrum of the solution (v) after a brief bubbling of air.

Determination of apparent formation constant β_2' of $[Cu^{I}(Fs)_2]^{3-}$ by direct metal titration

The experiments outlined in Figures 2c and 4 allowed definition of conditions for robust determination. Firstly, to avoid complications due to Cu(I) binding by other ligands, all known weak Cu(I) ligands such as Cl^- and MeCN were excluded carefully from the working solutions. Secondly, to avoid oxidation by trace dioxygen, the experiments were performed under anaerobic conditions in the presence of protective reductants NH_2OH (2.0 mM) and Asc (1.0 mM). Thirdly, to increase sensitivity and reliability, the effects of dilution were assessed carefully. Eqns 1 and 2 indicate that dilution of a system in equilibrium will lead to partial dissociation of $[Cu^{I}L_2]^{3-}$ to reach a new equilibrium to satisfy eqns 1-4. This principle is illustrated graphically in Figure S3. At a high total ligand concentration of [L] = 120 μM, the predicted titration curves are essentially indistinguishable when log $\beta_2 > 12$, but may become separated when $[L]_{tot}$ is lower (Figure S3). This principle was employed to consolidate the β_2' value determined for $[Cu^{I}(Fs)_2]^{3-}$ in Figure 2c. To this end, a set of solutions containing the same total concentrations of Fs (110 μM) and varying total concentrations of Cu (10-100 μM) was prepared in reducing buffer A under anaerobic conditions. Subsequent sets were generated by, respectively, two- and four-fold dilutions of the first set with buffer A. The absorbances of each set (after anaerobic transfer) were recorded after incubation for ~ 4 h. The experimental data of each set of solutions with $[Cu]_{tot}/[L]_{tot} < 0.6$ (filled circles) were fitted satisfactorily ($R > 0.99$) to eqn 5 to generate a consistent β_2' value of 1.0(2) x 10^{11} M^{-2} (Figure S4). This estimate consolidates the value of 1.2(2) x 10^{11} M^{-2} derived from the experimental data in Figure 3c. However, the experimental data from solutions with high apparent free Cu content (i.e., $[Cu]_{tot}:[L]_{tot} > 0.6$; Figures S4a,b, empty circles) cannot be fitted to eqn 5. Apparently, an increase in total Cu concentration in these cases did not result in an increase in the apparent 'Cu^{+}_{aq}' concentration in solution. The intrinsic instability of Cu^{+}_{aq} to oxidation, disproportionation and substitution means that higher concentrations of this metal ion in aqueous buffers are not sustainable, even under anaerobic and reducing conditions and in the absence of competing ligands.

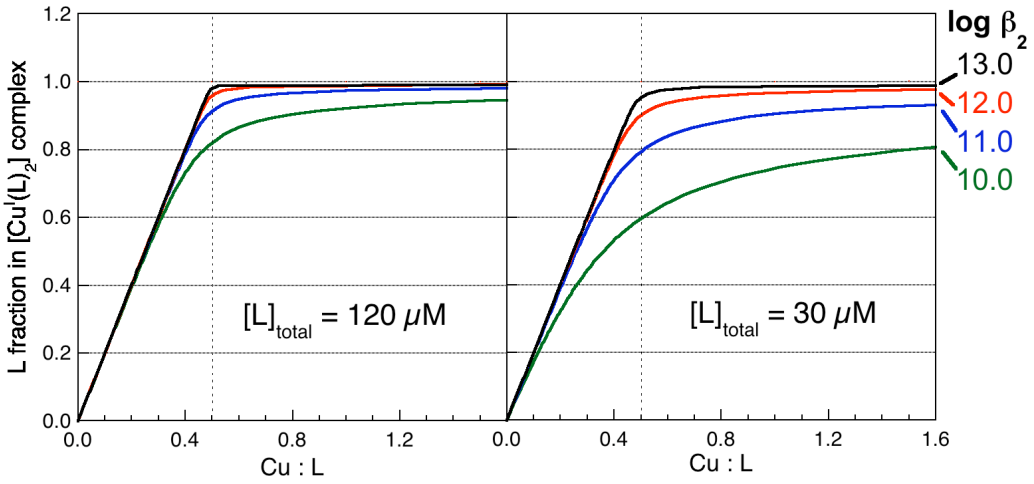

Fig S3. Calculated binding curves according to eqn 5. With $[L]_{total}$ = 120 μM, the curves are essentially indistinguishable when log β_2 > 12, but may become partially resolved when the $[L]_{total}$ is diluted considerably.

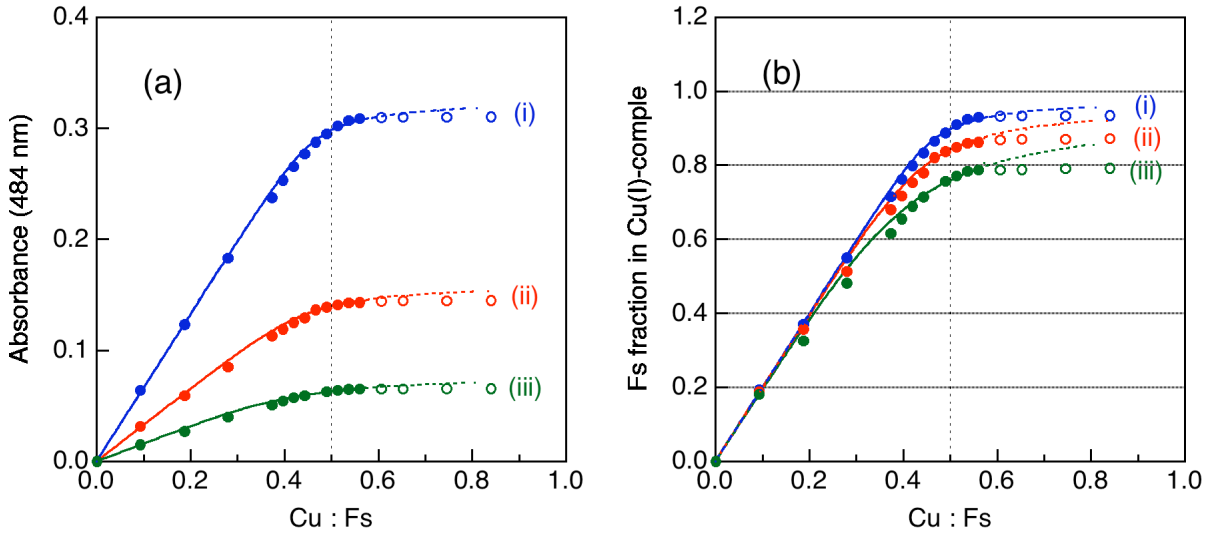

Fig S4. Determination of apparent formation constant β_2' of $[Cu^I(Fs)_2]^{3-}$ by direct metal titration in buffer A: (a) Variation of A_{484} for $[Cu^I(Fs)_2]^{3-}$ with change in molar ratio Cu:Fs with a fixed total [Fs] = 110 μM (i), 55 μM (ii) and 27.5 μM (iii). Sets of solutions (ii) and (iii) were prepared by two- and four-fold dilution of the set of solutions (i), respectively. (b) Conversion of the experimental data in (a) to an expression of ligand fraction in formation of $[Cu^I(Fs)_2]^{3-}$. Dilution of solutions (i) to solutions (ii, iii) led to partial dissociation of the metal complex. The traces shown are the best fits (R > 0.99) to eqn 5 of each of the three sets of experimental data which generated formation constants β_2' for $[Cu^I(Fs)_2]^{3-}$ = (0.88, 1.06, 1.06) x 10^{11} M^{-2}, respectively.

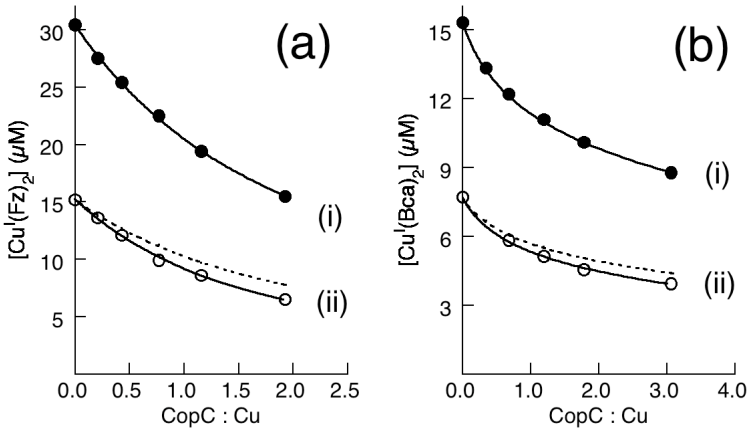

Fig S5. Determination of the Cu(I) binding affinity of CopC in buffer A under competing conditions with probes: (a) $[Cu^{I}(Fz)_2]^{3-}$ plus Fz ($[Cu]_{tot}$ ~ 30 μM and $[Fz]_{tot}$ = 300 μM) and (b) $[Cu^{I}(Bca)_2]^{3-}$ plus Bca ($[Cu]_{tot}$ ~ 15 μM and $[Bca]_{tot}$ = 40 μM). In each case, a stepwise increase in protein concentration in the solution led to a stepwise decrease in the spectral intensity of $[Cu^{I}(L)_2]^{3-}$, signifying a Cu^{I} transfer from $[Cu^{I}(L)_2]^{3-}$ to the added protein. The experimental data points for the originally prepared solutions are shown in solid circles and those for solutions obtained by a 1:1 dilution are shown in empty circles. Best fittings of the experimental data sets (i) and (ii) to eqn 9 (shown in solid traces) generated $K_D = 10^{-12.1}$ M in (a) and $K_D = 10^{-12.2}$ M in (b). The dash traces in (ii) are the simple 1:1 dilution curves of data sets (i).

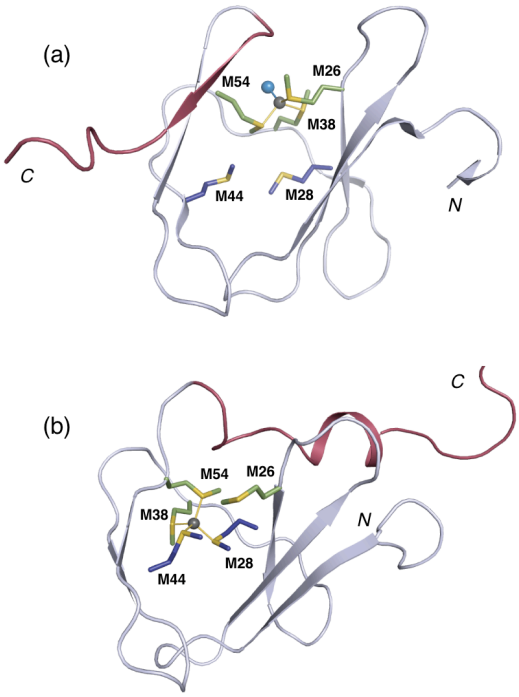

Fig. S6 Alternative Cu(I) sites 3S and 4S in CopK: (a) 3S site in the X-ray crystal structure of Cu^{I}-CopK (3DSO); (b) 4S site in the NMR structure of Cu^{I}-CopK (2KM0). Adapted with permission from ref 44. Copyright 2010 American Chemical Society.

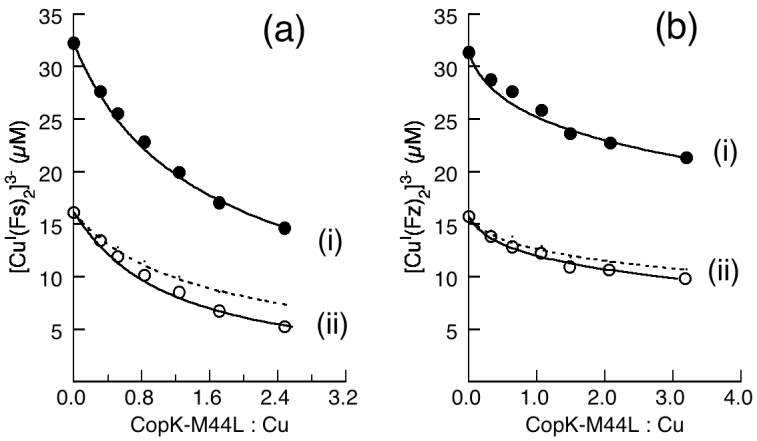

Fig S7. Determination of the Cu(I) binding affinity of Cu^I-CopK-M44L in buffer A under competing conditions with probes: (a) $[Cu^I(Fs)_2]^{3-}$ plus Fs ($[Cu]_{tot}$ ~ 32 μM and $[Fs]_{tot}$ = 120 μM) and (b) $[Cu^I(Fz)_2]^{3-}$ plus Fz ($[Cu]_{tot}$ ~ 31 μM and $[Fz]_{tot}$ = 70 μM). In each case, a stepwise increase in protein concentration in the solution led to a stepwise decrease in the spectral intensity of $[Cu^I(L)_2]^{3-}$, signifying a Cu^I transfer from $[Cu^I(L)_2]^{3-}$ to the added protein. The experimental data points for the originally prepared solutions are shown in solid circles and those for solutions obtained by a 1:1 dilution are shown in empty circles. Best fittings of the experimental data sets (i) and (ii) to eqn 9 (shown in solid traces) generated $K_D = 10^{-9.9}$ M in (a) and $K_D = 10^{-9.7}$ M in (b). The dash traces in (ii) are the simple 1:1 dilution curves of data sets (i).